JEE Journal of Ecological Engineering

Journal of Ecological Engineering, 2025, 26(6), 48–61
https://doi.org/10.12911/22998993/201995
ISSN 2299–8993, License CC-BY 4.0

Received: 2025.02.02
Accepted: 2025.04.05
Published: 2025.04.15

Controlled-release pesticide nanofibers for sustainable agriculture: Effects of processing parameters on fiber morphology and release kinetics

Vu Anh Doan[1], Le Thanh Hai Anh[1], Tuan Anh Phung[1], Duc Minh Vu[1], Vu Tran Khac[2], Liem Thanh Nguyen[1*]

[1] School of Material Science and Engineering, Hanoi University of Science and Technology, Hanoi, Vietnam
[2] School of Chemistry and Life Science, Hanoi University of Science and Technology, Hanoi, Vietnam
* Corresponding author's e-mail: liem.nguyenthanh@hust.edu.vn

ABSTRACT

This study aimed to develop a controlled release system for the carbamate insecticide fenobucarb using poly (lactic acid) (PLA) nanofibers produced by coaxial electrospinning. The objective was to produce core-shell nanofibers and evaluate their properties and fenobucarb release behaviour through several analytical techniques, including water contact angle measurements, scanning electron microscopy, transmission electron microscopy, and high-performance liquid chromatography. The optimal parameters for electrospinning were found as 8 wt.% PLA for the shell, 98 wt.% fenobucarb for the core, with shell feed rates of 0.6 mL/h and 0.18 mL/h for the core, using an applied voltage of 16 kV and a tip-to-collector distance of 16 cm. The finished nanofibers contained up to 74.713% fenobucarb by weight, with a gradual release of 12.7% after one week and 66.12% after three months. These findings demonstrate the potential of fenobucarb/PLA nanofibers as a viable method for extended and controlled pesticide delivery, which could enhance long-term pest management effectiveness while reducing pesticide usage. This reduction not only minimizes environmental impact but also supports the development of a greener and more sustainable agriculture.

Keywords: polylactic acid, fenobucarb, coaxial electrospinning, nanofiber, core feed rate.

INTRODUCTION

As global agriculture continues to advance, the use of fertilizers and pesticides has significantly increased, underscoring the need for their precise and efficient application. This is essential not only for enhancing crop yields and ensuring high-quality produce but also for mitigating the environmental and health impacts associated with their use [Pouladchang et al., 2021].

Synthetic pesticides play a crucial role in crop protection. However, their benefits are counterbalanced by considerable drawbacks. Improper application can lead to diminished effectiveness and contribute to severe environmental issues. The uncontrolled use of pesticides is linked to a host of problems, including the development of pest resistance, the demise of beneficial organisms, and the persistence of pesticide residues in water, soil, food, and living organisms. These challenges have driven researchers worldwide to develop innovative solutions that meet the nutrient demands of plants throughout their growth stages while minimizing financial losses and environmental damage [Liang et al., 2019; Songling et al., 2018; Qi et al., 2019].

In recent years, the focus has shifted towards developing innovative pesticide delivery systems within the field of agricultural biotechnology. These new systems aim to offer long-term protection from pests with minimal applications, improve the efficacy of active ingredients, and protect natural resources. One of the most promising advancements in this area is the utilization of polymers. Polymers enhance the solubility, stability, and controlled release of pesticides,

addressing agricultural needs more effectively while reducing environmental footprint [Sushila et al., 2021; Díaz et al., 2008].

Controlled-release pesticide systems typically consist of a polymer matrix that encapsulates chemical agents. These systems are engineered for the gradual diffusion of active ingredients through the polymer shell, ensuring targeted delivery at controlled rates. The shift towards biodegradable polymers, particularly Poly (lactic acid) (PLA), is highlighted in response to global plastic waste management challenges [Yin et al., 2017]. PLA's adaptability has been capitalized upon in recent research, focusing on enhancing its processing techniques and broadening its applications in biocomposites [Ghanmi et al., 2024].

Significantly, the role of nanotechnology in these advancements is underscored, with electrospinning featured as a prominent method for producing nanoscale materials [Sonseca et al., 2012; Okutan et al., 2014]. Coaxial electrospinning, a specialized variant of traditional electrospinning, is discussed for its efficiency in creating core-shell and hollow fibers. This method facilitates the blending of multiple polymers, preserving their unique properties, which is ideal for controlled-release applications. The resulting nanofibers, with their enhanced surface-to-volume ratio, offer improved performance over traditional polymer-coated substrates, making them highly suitable for advanced controlled-release systems [Nguyen et al., 2012].

Coaxial electrospinning, a specialized variation of traditional electrospinning, has emerged as an excellent technique for producing core-shell and hollow fibers. This method allows the blending of multiple polymers while preserving their individual properties, making it highly suitable for controlled-release applications. Nanofibers produced by this method have a much higher surface-to-volume ratio compared to traditional polymer-coated substrates, making them ideal for controlled-release systems. While electrospun nanofibers have been extensively researched for biological and pharmacological applications, their potential in agriculture specifically as carriers for controlled-release pesticide delivery has garnered relatively little attention. This study aims to explore the use of electrospun nanofibrous mats, particularly PLA fibers, as carriers for Fenobucarb, a carbamate insecticide, to create a controlled-release system that improves pesticide efficacy and sustainability in agricultural applications.

This research aims to develop a controlled-release system that not only improves the efficacy of pesticide delivery but also enhances the sustainability of agricultural practices by leveraging the unique properties of nanofibers produced via electrospinning. This approach represents a significant stride towards integrating sophisticated nanotechnological advances with practical agricultural applications. Fenobucarb (FNC), chemically known as 2-sec-butylphenyl-N-methylcarbamate, is a carbamate class insecticide predominantly employed in the agriculture sector. It is particularly vital in the cultivation of rice, where it combats pests like plant hoppers and leaf hoppers. Fenobucarb functions by inhibiting acetylcholinesterase, an enzyme essential for nerve function in insects, thereby disrupting their neurological processes and ultimately leading to their demise [Kumar et al., 2025].

While Fenobucarb is effective in pest eradication, its application is not devoid of environmental concerns. The primary issues include the potential for water source contamination and adverse effects on non-target organisms. These environmental risks have prompted researchers to investigate alternative, more sustainable pest control methods. Fenobucarb can cause a range of side effects as a cholinesterase inhibitor. Potential effects include acute toxicity symptoms such as nausea, vomiting, dizziness, headache, excessive salivation, sweating, muscle weakness, and respiratory distress. In severe cases, exposure can lead to convulsions, loss of consciousness, and even death due to respiratory failure. Chronic exposure may cause neurological issues, liver damage, or endocrine disruption. Skin and eye irritation are also possible if there is direct contact. Proper protective measures should be taken when handling fenobucarb to minimize risks.

The direct use of FNC by farmers can have several negative impacts on water environments. As FNC quickly seeps into the soil, it can contaminate groundwater, degrade water quality, and affect aquatic ecosystems. Additionally, since FNC is washed away before fully exerting its effects on pests, its effectiveness in pest control is significantly reduced. This may lead farmers to use more FNC, increasing the risk of environmental pollution and posing potential health hazards to humans. For this reason, the development of pesticides containing FNC with a controlled release

rate as desired will enhance the effectiveness of this active ingredient. At the same time, it will help minimize negative impacts on soil and water environments, as well as reduce health risks for farmers during use.

Among the promising advancements are controlled-release systems that incorporate biodegradable polymers. These systems aim to minimize environmental impact and enhance the efficacy of pesticide applications by extending the active period of the pesticide's release. One particularly effective method for creating these controlled-release systems is electrospinning, which has been shown to sustain and prolong the activity of pesticides [Jenildo Santos Silva Junior et al., 2015; Laura E. Sperling et al., 2016]. Although research in electrospinning for Fenobucarb's controlled release is still emerging, recent studies have made significant progress. This study details the first successful attempt to fabricate electrospun nanofibers using PLA with varied concentrations of Fenobucarb.

This research explored the potential of these nanofibers to serve as a controlled-release mechanism for pesticides, providing a novel and efficient approach to pest control that could revolutionize agricultural practices by reducing environmental impacts and improving sustainability.

MATERIAL AND METHODS

Materials

Polylactic acid, product code: Resomer@ R203H (M_W 18.000-24.000, Tg: 48–52 °C) was purchased from Sigma-Aldrich; Chloroform (≥ 99%) and N, N-dimethylformamide (> 99.5%) and Toluene (99.7%) were supplied by Xilong Scientific Co., Ltd., China; Fenobucarb (98%) was purchased from DC Chemical Co., Ltd., China. All chemicals were used without any purification. All the chemicals were used without any purification.

Preparation of FNC/PLA nanofiber scaffolds

For the shell solution, PLA was dissolved in a chloroform/N, N-dimethylformamide (CHF/DMF) solvent mixture with a weight ratio of 75/25. The concentration of PLA was varied at 6.0 wt.%, 8.0 wt.%, 10.0 wt.%, and 12.0 wt.% to assess the impact of these concentration levels on the resulting fiber characteristics. The PLA solution was subjected to continuous magnetic stirring for one hour at 50-55 °C to ensure complete dissolution of the PLA. The core solution consisted of a Toluene solvent mixed with varying concentrations of the active agricultural component at 50%, 70%, 90%, and 98.0% wt./wt. of FNC (a.k.a. Standard Fenobucarb). Then, the above solutions were transferred to a 5 mL syringe with a steel needle. In the electrospinning process, coaxial spinneret was utilized to fabricate core-shell fibers. The inner needle (30G) had inner and outer diameters of 0.16 mm and 0.31 mm, respectively, while the outer needle (21G) had inner and outer diameters of 0.51 mm and 0.82 mm, respectively.

The effects of applied voltages on the electrospinning process were assessed at 14, 16, and 18 kV. High voltage forces the polymer jet from the needle towards the collector, with distances of 16 to 20 cm.

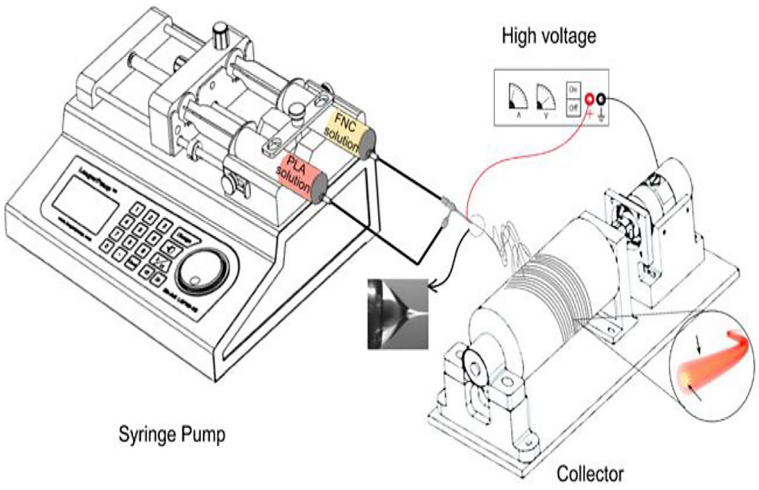

Figure 1. Schematic view of coaxial electrospinning process

The flow rate for the PLA shell solution was fixed at 0.6 mL/h during the procedure, whereas the core solution flow rate was changed between 0.15 and 0.22 mL/h. The optimal conditions used to produce the fibers presented here were at room temperature (25 ± 2 °C) and moderate humidity (50%). A schematic view of the coaxial electrospinning process is shown in Figure 1.

Characterization of solutions and FNC/PLA scaffolds

The viscosities of the PLA and FNC solutions were measured using a Brookfield DV-E digital viscometer with LV-2 spindle at 100 rpm and 25 °C according to ASTM -D2196. The reported viscosity for each solution was the average of five measurements.

The electrical conductivities of PLA and FNC solutions were measured at 25 °C using a conductivity meter (MeterLab CDM210, Radiometer Analytical - France).

The nanofiber morphology was evaluated using scanning electron microscopy (SEM). The SEM images were analyzed with ImageJ software as an imaging tool, to measure the average fiber diameter and assess its distribution across the samples. For statistical accuracy, 100 fibers were randomly selected for analysis.

The core-shell structure of FNC/PLA nanofibers was analyzed using a transmission electron microscope - TEM (JEM 2100, Jeol, Japan) operating at an electron acceleration voltage of 200 kV. For this analysis, samples of the nanofibers were prepared by electrospinning FNC/PLA solutions directly onto copper grids coated with a carbon film. This process took approximately 5 seconds. The prepared grids were then examined with the TEM, where electron beams were transmitted through the samples to capture detailed images of the core-shell structures. Since the electron beams must pass through the full diameter of the nanofibers, the analysis was limited to fibers with diameters smaller than 300 nm to accurately visualize the core-shell structure.

TGA experiments of the FNC/PLA nanofiber and pristine PLA were performed under an N2 atmosphere and heated from 35 °C to 450 °C with a heating rate of 10 °C min^{-1} using a Discovery TGA 550 (TA Instruments, USA) equipment.

Attenuated total reflectance Fourier-transformed infrared spectroscopy (ATR-FTIR) was used to analyze neat PLA and FNC/PLA nanofiber mats using the Nicolet iS20 machine. The spectra were recorded over a wavenumber range of 4000 to 500 cm^{-1} using 64 scans and a resolution of 4 cm^{-1}. The analysis aimed to investigate the structural and property differences among the obtained fibers.

The hydrophilicity of nanofiber mats was tested using the contact angle system, based on the sessile drop technique. Three replicates were tested in different areas for each sample. The average of these measurements was used to determine the WCA, calculated from photographs using ImageJ software.

The total amount of the FNC contained in the nanofiber mats was quantified using High-Performance Liquid Chromatography (HPLC) (Thermo Scientific Nicolet Ltd., USA).

All the results were presented as the mean and standard derivation (SD) of replicate studies. One-way analysis of variance (one-way ANOVA) was used to compare the means by factor levels, and $p < 0.05$ was considered significant.

Release behaviour studies

Determination of loading capacity

10 mg of FNC-loaded samples were randomly cut from fabricated mats and dissolved in 10 mL Chloropicrin using an ultrasonic bath until the solutions became completely homogeneous. Samples were analyzed by High-Performance Liquid Chromatography (HPLC) to determine the amount of FNC in the nanofiber mats. The pesticide loading capacity (LC %) of core-shell fiber membranes was evaluated using the following Equation 1 below.

$$\frac{\textit{The total FNC content encapsulated in fibers}}{\textit{The initial weight of the tested sample}} \times 100 \quad (1)$$

In vitro pesticide release

The in vitro release ability of FNC/PLA core/shell fibers was investigated by immersion in deionized water for over 30 days at approximately 40 °C. Specimen (1×1 cm, weight 10 mg) was cut at random from core-shell fiber membranes. Then, each specimen was placed in a bottle containing 40 mL of deionized water. HPLC spectrophotometer was used to analyze the solution at different times ranging from 1 to 12 weeks. Samples will be taken every 7 days to determine the amount of pesticide released from the fiber mats. The final results show the total amount of FNC

released from the specimens at various immersion times. The cumulative release data was used to represent the pesticide release as a function of time, in Equation 2.

$$Release\ (\%) = \frac{M_t}{M_\infty} \times 100 \qquad (2)$$

where: Mt is the amount of FNC released at time t, $M\infty$ is the total amount of FNC in the nanofiber mat.

RESULTS AND DISCUSSION

Effect of processing parameters on fiber morphology

The effect of PLA shell solution concentration

The initial processing parameters were defined as follows: the shell solution concentration (PLA) was maintained at 8 wt.%, with a shell feed rate of 0.6 mL/h, a core solution concentration of 50%, and a core feed rate of 0.18 mL/h. The tip-to-collector distance (TCD) was set at 16 cm, and an applied voltage of 16 kV was used. The viscosity and conductivity of both the core and shell solutions were measured to evaluate their impact on fiber formation, fiber diameter, and other associated processing parameters. The ejection of a thin polymer jet occurs when the electric force on induced charges within the polymer liquid surpasses surface tension. This charged jet is elongated, accelerated under the hight electric field, and subjected to various instabilities before drying and depositing onto a substrate as a random nanofiber mat. Table 1 presents the viscosity and electrical conductivity values for the PLA and FNC solutions. As shown in Table 1, the PLA and FNC solutions exhibit notably low electrical conductivities, a characteristic attributed to the insulating properties of polymers.

Table 1. Viscosity and electrical conductivity of PLA and Fenobucarb solutions

Solution	Viscosity, cP	Conductivity, μS/cm
PLA 6%	112.7	6.10
PLA 8%	114.2	5.78
PLA 10%	123.6	5.23
PLA 12%	129.1	5.05
Fenobucarb 50%	67.3	6.96
Fenobucarb 70%	132.1	5.02
Fenobucarb 90%	534.6	2.56
Fenobucarb 98%	1026.1	0.58

The viscosity of the PLA and FNC solutions showed minimal variation when the FNC concentration was below 70%. However, significant differences in viscosity were observed at higher FNC concentrations (90% and 98% in this study), showing the influence of concentration on the shell/core solutions. Fiber formation was found to be strongly influenced by the electric field acting on the shell solution's surface. In cases of poor electrical conductivity, particularly in high concentration core solutions, the solution concentration significantly affected the resulting fiber properties, such as shape and diameter, necessitating corresponding adjustments to the processing parameters. The morphology of the fibers under varying shell solutions was analyzed using Scanning Electron Microscopy (SEM). Figure 2 shows the core/shell fibers formed a randomly interconnected fibrous structure with smooth surfaces. The fiber size demonstrated variability in response to adjustments in the shell solution during the fabrication process.

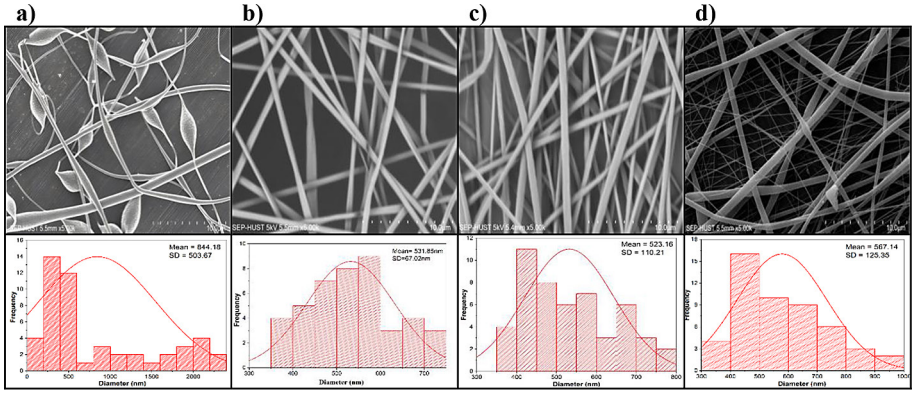

Figure 2. SEM images and distribution of diameters of FNC/PLA nanofibers at different shell solution concentrations: (a) 6.0 wt.%; (b) 8.0 wt.%; (c) 10.0 wt.%; (d) 12.0 wt.%

As shown in Figure 2, fiber formation faces difficulties at a low PLA concentration of 6 wt.% (Figure 2.a), with numerous defects (beads) and a high standard deviation in fiber diameter (SD = 503.86). At a PLA concentration of 8 wt.% (Figure 2.b), the electrospun fibers exhibit a uniform and consistent morphology, indicating optimal conditions for fiber fabrication. However, increasing the PLA concentration beyond 8 wt.% (to 10 wt.% and 12 wt.% in this study) alters the nanofiber structure, transitioning from cylindrical to flattened shapes and reducing the yield.

These results indicate that a critical PLA concentration is required to achieve bead-free and uniform fibers. Excessively high concentrations lead to the drying of the polymer solution at the needle tip, blocking flow and hindering fiber production.

The effect of applied voltage

The applied voltage plays an important role in the electrospinning process. Figure 3 and Table 2 illustrate the morphology, diameter, and standard deviations of FNC/PLA nanofibers at voltages between 14 and 20 kV. At 14 kV (Figure 3.a), the produced nanofibers were large, uneven, and contained numerous beads in the fiber mats, with a high standard deviation (SD = 153.38). At 16 kV (Figure 3.b), the nanofibers displayed uniform diameters and a low standard deviation (SD = 54.63), indicating optimal conditions for nanofiber formation. However, at higher voltages of 18 kV and 20 kV (Figures 3c and 3d), the fibers became flat and exhibited poor morphology. This can be attributed to the instability of fibers caused by excessive voltage, where the electrospinning process becomes discontinuous, and the electrostatic repulsion between the needle and the collector destabilizes the fiber formation. High voltage accelerates fiber motion toward the collector drum, leading to overstretching, incomplete solvent evaporation, and flat fiber shapes. Additionally, overstretching may induce surface cracks in the fibers. The data in Table 2 shows that increasing the applied voltage above 16 kV leads to a noticeable increase in both fiber diameter and standard deviation. This can be attributed to the faster ejection rate of the shell solution at higher voltages, resulting in a greater volume of resin being extruded and producing larger fibers. Moreover, higher voltages tend to stretch polymer chains with lower molecular weights more effectively, while higher molecular weight chains resist stretching, causing greater variability in fiber diameter.

The observed disparity in the stretching behaviour of polymer chains underscores the limitations of increasing voltage to improve fiber uniformity. Due to the low electrical conductivity of both the shell and core solutions, voltage adjustments are effective only within a certain range to ensure proper fiber deposition on the collector. Beyond 16 kV, further increases in voltage have minimal positive impact. As a result, 16 kV was identified as the optimal voltage for the next study.

The effect of the needle tip-to-collector distance

The distance between the needle tip and collector (TCD) influences the solvent evaporation rate in polymer solutions, allowing sufficient time for fibers to form before deposition on the drum collector [17]. Figure 4 presents micrographs of FNC/PLA electrospun fibers produced at varying TCDs: 14, 16, 18, and 20 cm. The morphology of

Table 2. Distribution of diameters of FNC/PLA nanofibers at different applied voltages

Applied voltages, kV	Mean diameter, nm	Standard deviation
14	570.01	153.38
16	543.18	54.63
18	546.05	67.02
20	531.85	63.34

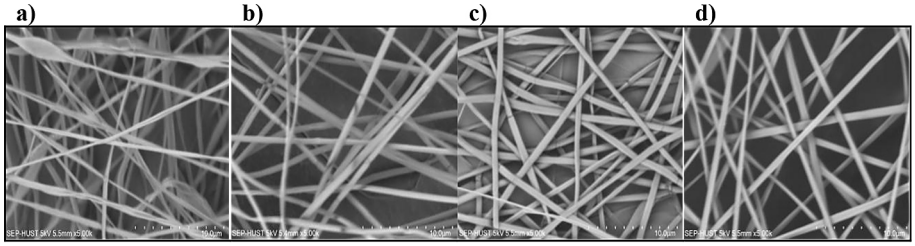

Figure 3. SEM images of FNC/PLA nanofibers at different applied voltages: (a) 14 kV; (b) 16 kV; (c) 18 kV; (d) 20 kV

nanofibers remained consistent across TCDs of 14 to 20 cm, producing continuous fibers with varying standard deviations. However, at 18 cm and 20 cm (Figures 4c and 4d), beads and twisted fibers appeared. This can be attributed to excessive TCDs, where overstretched fibers harden near the collector due to prolonged travel distance, evaporation, and electric force-induced stress.

Table 3 shows the diameter and standard deviations of FNC/PLA nanofibers with TCDs ranging from 14 cm to 20 cm. The results further highlight that a TCD of 16 cm yields nanofibers with the smallest and most uniform diameters. These fibers measured between 300 nm and 600 nm, with an average diameter of 543.18 nm and a standard deviation of 54.63, representing optimal conditions for fiber formation.

The data in Table 3 also shows that increasing the tip-to-collector distance (TCD) from 16 cm to 20 cm has minimal impact on fiber diameter or standard deviation. To achieve optimal conditions for producing uniform and smaller nanofibers, a TCD of 16 cm was selected for further studies

The effect of core feed rate

In the electrospinning technique, electrical charges are localized on the shell solution's outer surface, leaving the core solution unaffected by the electric potential. The stretching of the shell solution by electrostatic forces exerts a drag on the core solution, enabling the incorporation of non-spinnable materials as core components in nanofiber production. The feed rate plays a vital role in maintaining the balance between the supply of the solution and the evaporation of the solvent under the influence of the electric field, making it a critical parameter for controlling fiber formation. Figure 5 and Table 4 show SEM images and distribution of diameters of FNC/PLA fibers at different core feed rates. SEM images of FNC/PLA core/shell electrospun fibers fabricated under core solution feed rate ranging from 0.16 to 0.22 ml/h.

As shown in Figure 5, changes in the core feed rates significantly affect the shape, morphologies,

Table 3. Distribution of diameters of FNC/PLA nanofibers at different TCDs

TCD, cm	Mean diameter, nm	Standard deviation
14	512.73	72.48
16	543.18	54.63
18	511.81	75.73
20	558.47	81.46

Table 4. Distribution of diameters of FNC/PLA nanofibers at different core feed rates

Core feed rate, mL/h	Mean diameter, nm	Standard deviation
0.16	604.28	96.95
0.18	543.18	54.63
0.20	712.57	114.63
0.22	747.87	132.01

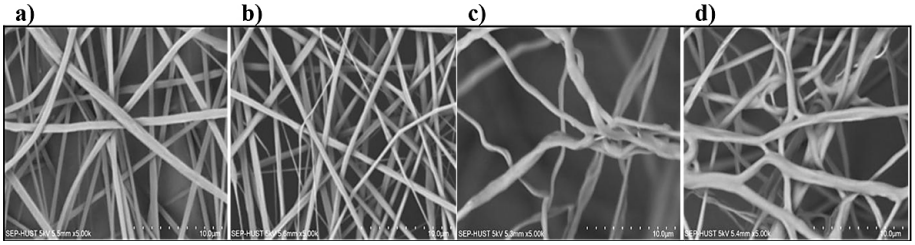

Figure 5. SEM images of FNC/PLA fibers at different core feed rates: (a) 0.16 mL/h; (b) 0.18 mL/h; (c) 0.20 mL/h; (d) 0.22 mL/h

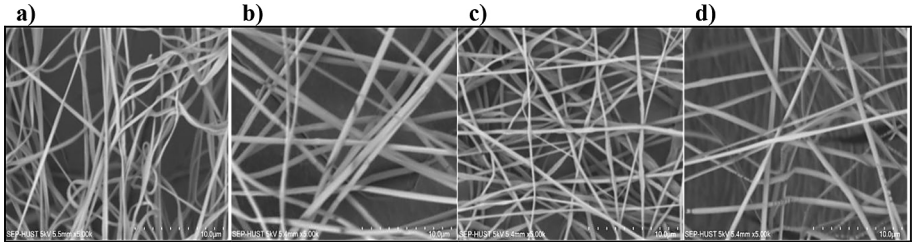

Figure 4. SEM images of FNC/PLA fibers at different TCDs: (a) 14 cm; (b) 16 cm; (c) 18 cm; (d) 20 cm

and outer diameters of the nanofibers. An increased core feed rate resulted in fibers with larger outer diameters. Increasing the core feed rate from 0.18 mL/h to 0.22 mL/h resulted in a significant increase in the average fiber diameter, rising from 525.74 nm to 712.57 nm, corresponding to a 35.5% increase. This was accompanied by a notable rise in the diameter standard deviation, from 46.46 to 132.01.

Moreover, the fiber morphology shifted from a circular cross-section to a flattened structure. This phenomenon is attributed to the low viscosity of the core solution (67.3 cp), due to its high solvent content (50%), compared to the PLA shell's higher viscosity (114.2 cp). The increased core feed rate likely introduced a greater volume of core solution into the fibers, preventing complete solvent evaporation. The residual solvent influenced the fiber diameter and morphology and promoted adhesion between fibers. The core feed rate of 0.18 mL/h was chossen for the next studies.

The effect of FNC concentration

The results presented in Table 1 indicate that as the concentration of FNC increases, the viscosity of the solution rises significantly, accompanied by a reduction in electrical conductivity. During the electrospinning process, the electric field exerts a force that draws the solution into fibers. Consequently, it is evident that viscosity and electrical conductivity play a critical role in determining the morphology of the fabricated microfibers and the core content in fibers (Figure 6).

This study focused more on the FNC concentration to evaluate the product's subsequent properties in the practical applications of FNC/PLA nanofiber membranes. Maintaining PLA concentration at 8 wt.% while the FNC concentration varying from 50% to 98% revealed a direct correlation: as the FNC concentration increased, so did the nanofiber diameter. Figure 7 shows the morphology of FNC/PLA core/shell fibers fabricated

Figure 6. Digital images of PLA shell and different FNC solutions

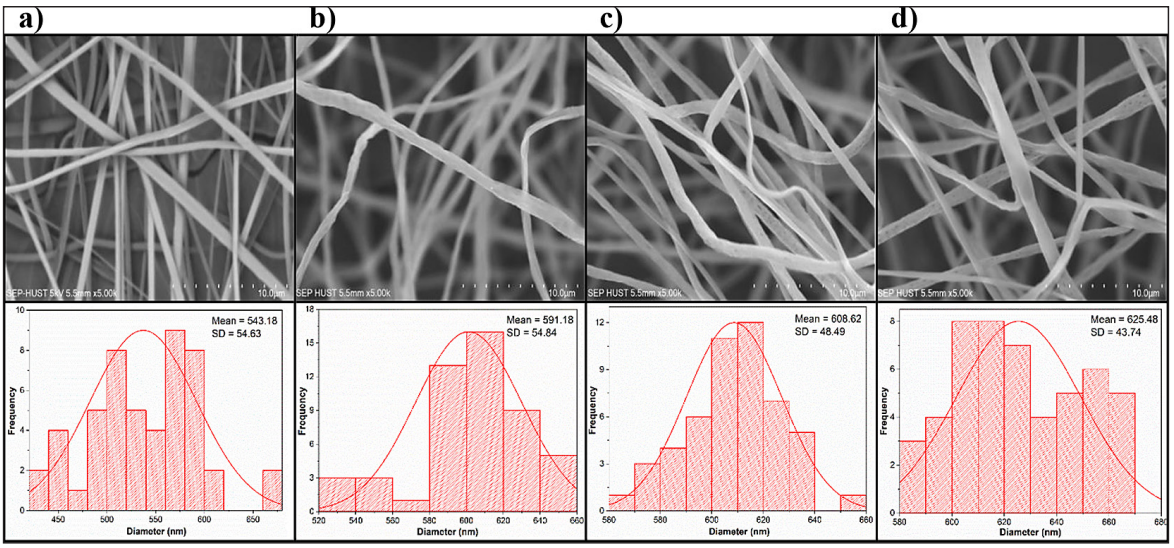

Figure 7. SEM images of (a) PLA fibers and FNC/PLA core/shell fibers at different FNC concentrations (b) 50%, (c) 70%, (d) 90% and (e) 98%

using co-axial electrospinning. It is observed that the fiber diameter gradually became larger, reaching over 600 nm. As the FNC concentration increased from 70% to 98%, the fiber diameter showed only a slight increase, rising from 591.18 nm to 625.48 nm, representing a 5.8% increment. Fiber diameter measurements were randomly sampled during fabrication. Notably, within the range of 90% to 98% FNC concentration, the standard deviation of the fiber diameter decreased. This trend is attributed to the effect of the solvent content in the core, which influences the solution's viscosity, electrical conductivity, and, consequently, the resulting fiber properties.

Transmission Electron Microscopy (TEM) images clearly revealed the core/shell structure and the distinct boundary between the two layers. These observations confirm the successful fabrication of FNC/PLA core/shell fibers and validate the intended configuration (Figure 8).

The outer PLA layer of the core/shell fibers exhibited surface porosity, attributed to solvent evaporation during the polymer jet drying process.

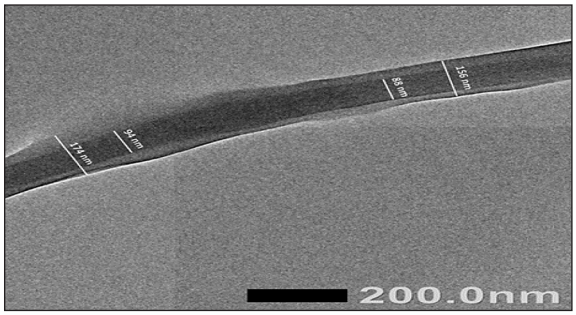

Figure 8. TEM image shows the core-shell structures of the FNC/PLA nanofiber

This porous structure acts as a potential channel for the release of active agents through diffusion and degradation mechanisms, playing a vital role in the controlled release of pesticides from the core/shell fibers. In designing this controlled-release system, the PLA shell functions as a physical barrier, facilitating pesticide release without relying on chemical crosslinking, which can pose environmental risks. Size uniformity is critical in fabricating microfibers containing FNC for slow-release functionality. To optimize FNC content within the fibers, a concentration of 98% was selected.

Chemical composition and thermal properties

FTIR measurements

The interaction between the two components is evident in the infrared spectrum, the characteristic peaks of PLA and FNC are shown in Figure 9. These peaks provide insights into the molecular structure and bonding interactions within the materials. Attenuated total reflectance Fourier-transform infrared spectroscopy (ATR-FTIR) was utilized to investigate the chemical surface characteristics of FNC/PLA nanofiber scaffolds. The spectra of pristine PLA, as shown in Figure 9, exhibited characteristic peaks at 2996 cm^{-1}, 1752 cm^{-1}, and 1182 cm^{-1}, corresponding to CH_3 stretching, C=O stretching, and -C-O-C stretching vibrations, respectively [K. KrishnaKumar et al., 2025]. In contrast, FNC displayed absorption peaks at 3311 cm^{-1}, 1710 cm^{-1}, and 1529 cm^{-1}, attributed to the stretching vibrations of amide A, amide I, and amide II groups, respectively [Jenildo

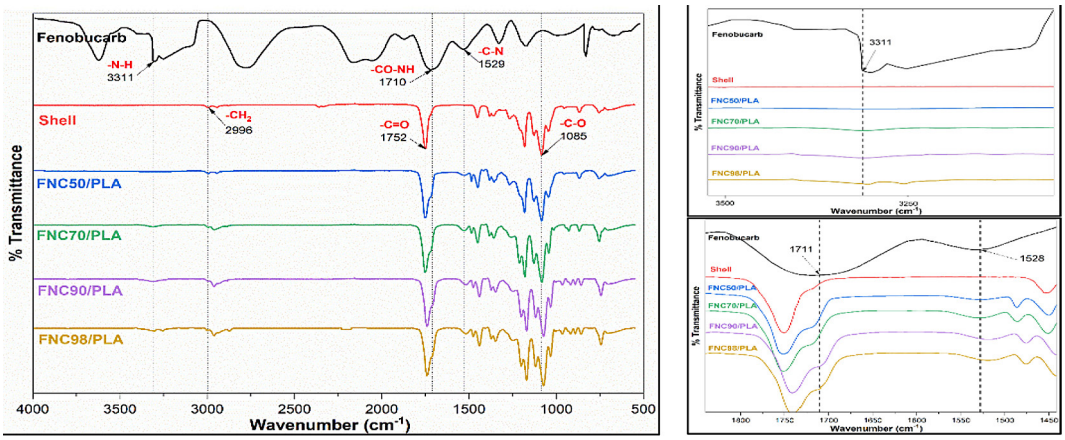

Figure 9. ATR-FTIR spectra of neat PLA, FNC, and fibers fabricated at different FNC concentrations; sample code: shell: PLA; FNC50/PLA: 50% FNC; FNC70/PLA: 70% FNC; FNC90/PLA: 90% FNC; FNC98%: 98% FNC in core

Santos Silva Junior et al., 2015]. The FTIR analysis of FNC/PLA core/shell nanofibers confirmed the presence of Fenobucarb functional groups (-CO-NH-, -CN, and -NH) on the fiber surface, with their intensities increasing proportionally to the FNC concentration in the core solution.

At higher core concentrations (above 70% FNC), the peak intensities were notably amplified, likely due to an increased core feed rate that promotes the migration of FNC molecules toward the fiber surface during the electrospinning process. This phenomenon enhances the detectability of FNC functional groups on the microfiber shell. The FTIR results unequivocally validate the successful incorporation of FNC pesticide within the fiber core.

Surface wettability properties

The water absorption capacity of pure PLA fibers and FNC/PLA core/shell fibers was evaluated through Water Contact Angle (WCA) measurements. Static water contact angle measurements were employed as shown in Figure 10. The presence of the -CH_3 group in PLA contributes to its good hydrophobicity. This characteristic creates favourable conditions for the controlled release of FNC, as the PLA shell acts as a barrier, preventing FNC in the core from releasing too fast.

As shown in Figure 10, the water contact angle exhibits significant variation with changes in the core concentration. The contact angle for pristine PLA was determined at 117.5°, serving as a baseline for comparison. In contrast, the contact angles for FNC/PLA nanofibers fabricated with different core concentrations were much lower, ranging from 89.4° to 84.2°. These findings demonstrate a notable reduction in the contact angle compared to pristine PLA, highlighting the impact of core concentration on the surface wettability of FNC/PLA nanofibers.

The contact angle of FNC/PLA nanofibers exhibits a decreasing trend with an increase in the core concentration. This can be explained by the increased core feed rate facilitating the migration of PLA resin to the surface of the PLA shell. The resultant exposure of FNC, the hydrophilic material, on the surface, combined with the formation of pores on the fiber structure and roughness of the fiber surface contributes to an increase in the hydrophilicity of the nanofibers. These observations are corroborated by the TEM image (Figure 8), which clearly demonstrates the surface morphology and chemical shifts indicative of this behavior.

Thermogravimetric analysis

Figure 11 displays the TGA analysis of the PLA, FNC, and FNC/PLA fibers. The results show that the degradation temperature of PLA fiber is 327.4 °C, and the decomposition of FNC occurs in two stages. The first stage dissolved at 75.6 °C, and the second at 202.5 °C. It has been noticed that the decomposing temperature of PLA decreases as the amount of FNC increases. This is because the byproduct of FNC decomposition promoted the degradation of PLA. The analysed samples show two major degradations: one from FNC thermal breakdown and the other from PLA decomposition. With the increase in the amount of FNC, the percentage of first thermal decomposition also increases. However, the PLA does not decompose below 100 °C, and the thermal decomposition temperature of PLA is higher than that of FNC, which has good stability. Thus, PLA is a good sustained-release material for FNC.

Evaluation of FNC loading

The results from Figure 12 demonstrate that the FNC content within the fibers exhibits substantial variation based on the FNC concentration in the core solution. The total amount of FNC in the nanofiber mat was quantified using HPLC analysis and calculated as shown in Equation (1). The loading of FNC pesticide fiber could be as high as 74.713% at a FNC concentration of 98%. The loading contents of FNC found in the fiber membranes

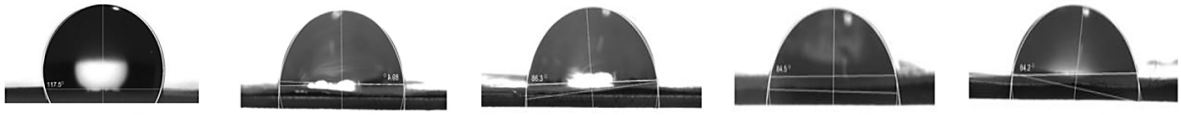

Figure 10. The images of water sessile drop on neat PLA and FNC/PLA fibers membranes at different FNC concentrations (50%; 70%; 90%; 98%)

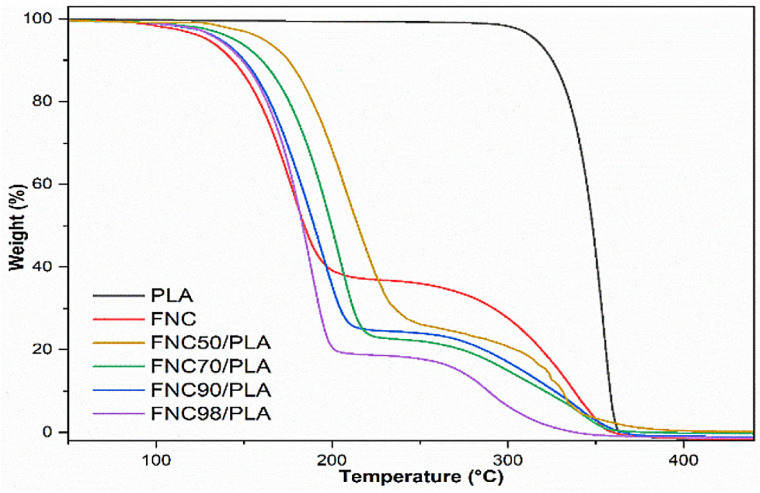

Figure 11. TGA analysis of PLA fiber and FNC/PLA fiber at different concentrations of FNC

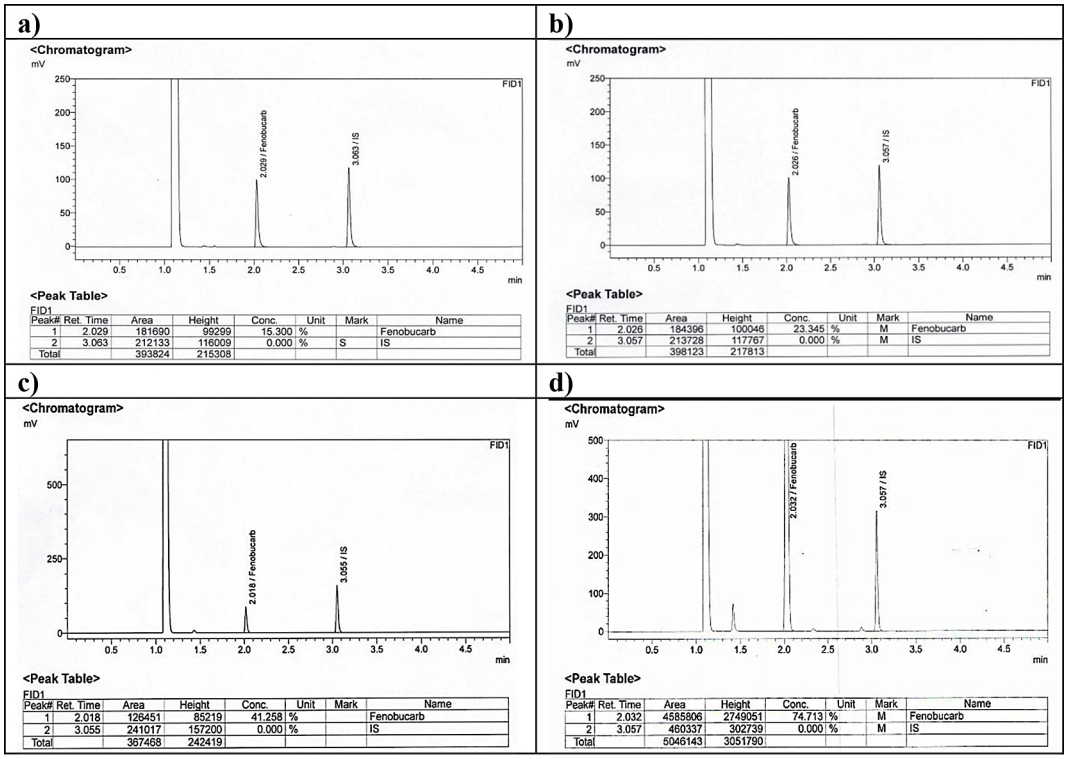

Figure 12. Fenobucarb loading content at different concentrations of FNC: (a) FNC50/PLA; (b) FNC70/PLA; (c) FNC90/PLA; (d) FNC98/PLA

showed some differences in comparison to their initial added values. At an initial concentration of 50% FNC, the fiber content is measured at 15.3%. Increasing the concentration to 70% results in an FNC content of 23.345%, reflecting a 52.6% increase. When the core solution concentration is further increased to 98%, the FNC content in the fibers reaches 74.713%, representing a significant 488.32% increase compared to the 50% concentration. This behaviour can be attributed to the loss of FNC due to solvent evaporation during the fiber formation process.

Release behaviour characteristics

Slow-release fertilizers are critical for improving nutrient utilization efficiency and reducing environmental impacts. European guidelines stipulate that, under standardized conditions of 25 °C, the nutrient release rate should be indicative of a

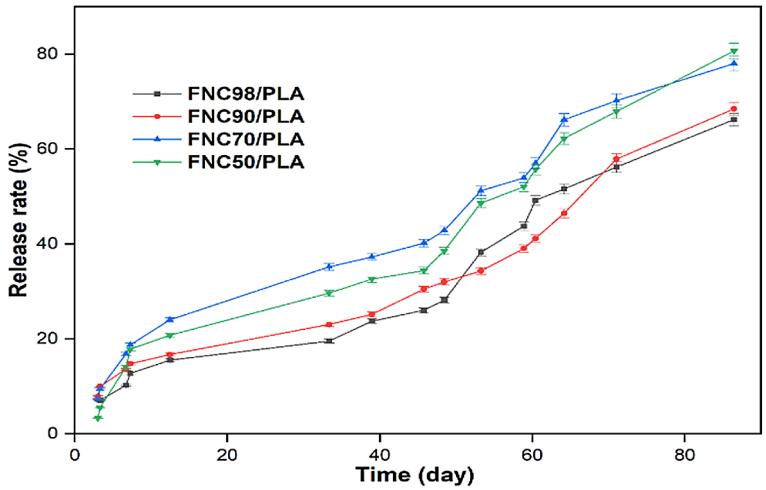

Figure 13. The release rate for FNC/PLA fibers in the natural environment

21-day gradual release period. Similarly, China's national standard, GB/T 23348-2009, requires monitoring nutrient release through immersion tests in aqueous solutions at 25°C, with an initial release rate of 80%.

The released weight of FNC was calculated using Equation 2. Figure 13 shows the Fenobucarb released rate of FNC/PLA nanofiber over a 24-day period. The release rate of FNC from the nanofibers ranged between 20% and 30% of the total encapsulated content. By 84 days, approximately 80% of the FNC was released. The release profile revealed an initial rapid breakdown of weakly bound FNC on the nanofiber surface, followed by a sustained release of the encapsulated pesticide from within the fibers. This biphasic release pattern underscores the stability and gradual release potential of the formulation.

A higher concentration of FNC in the core led to a decrease in the cumulative drug release and a faster saturation of the release process. The observed defects in the core-shell nanofibers, manifesting as holes post-water immersion, can be attributed to the initially high core flow rate. This occasionally prevented the PLA shell from completely encapsulating the core solution. Additionally, using the same solvent for both the core and shell made it more likely for the pesticide to dissolve during electrospinning. Therefore, modulating the flow rates during the formation of fibers can effectively control the release rate and amount of the drug from the core-shell nanofiber membraces.

Figure 13 also illustrates that the release rate of FNC over time is inversely proportional to the FNC content within the microfibers. The FNC98/PLA fibers exhibit the lowest release rate, achieving 63.5% after 84 days, whereas the FNC50/PLA fibers reach nearly 80%. However, this does not imply that the total amount of active compounds released from FNC50/PLA microfibers exceeds that of FNC98/PLA, as the FNC content within each type of microfiber differs.

CONCLUSIONS

Fenobucarb pesticide-loaded PLA fibers were successfully produced via co-axial electrospinning. This study identified the optimal conditions for producing core/shell coaxial electrospun fiber membranes. Optimal conditions were a shell solution concentration of 8 wt.%, a shell feed rate of 0.6 mL/h, a core feed rate of 0.18 mL/h, a needle tip to collector distance of 16 cm, and an applied voltage of 16 kV. All electrospinning processes were conducted at room temperature (25 ± 2 °C) and moderate humidity (50%). SEM and TEM analyses confirmed the core-shell structure, with shell average diameters of about 625.48 ± 43.74 nm at FNC concentration of 98%.

The results also show that processing parameters such as TCD, core/shell concentration, applied voltage all affect the properties of the resulting fibers. However, the values of the above parameters can fluctuate within a large range without much affecting the properties of the fibers such as diameter or standard deviation. Meanwhile, variations in core (FNC) concentration significantly affect FNC content in fibers. The nanofibers contained up to 64.561% fenobucarb by weight, with a gradual release of 12.7% after

one week and 66.12% after three months when using an FNC concentration of 98%.

The core/shell structure gives benefits such as preserving the bioactivity of plant nutrients, not requiring the use of chemical crosslinking agents, and facilitating controlled degradation and extended release of fertilizer. The concentration of fertilizer in the core solution is one of the crucial factors for determining the release quantity. Thus, the PLA-loaded FNC fiber membranes fabricated in this study hold promise for future agricultural applications and represent an advancement in the use of electrospinning technology within this field.

The fabrication of nanofibers with an outer shell made of PLA, a fully biodegradable plastic, and a core of FNC helps mitigate the limitations associated with the direct use of FNC. However, their future application may encounter certain challenges. The first challenge is the electrospinning fabrication technology, which has a low production efficiency, making large-scale manufacturing difficult. This limitation, however, can be overcome by increasing the number of nozzles on a single device or using multiple devices simultaneously. The biggest challenge is to develop a product that simultaneously ensures the effectiveness of the drug against pests while maintaining an appropriate release rate.

Acknowledgment

This research was supported by The Development Program of Basic Science in the Fields of Chemistry, Life Sciences, Earth Sciences, and Marine Sciences, Vietnam Ministry of Science and Technology, under Grant ĐTĐL.CN-111/21.

REFERENCES

1. Pouladchang A, Tavanai H, Morshed M, Khajhali J, Shamsabadi AS. (2021). Controlled release of thiram pesticide from polycaprolactone micro and nanofibrous mat matrix. *Journal of Applied Polymer Science, 139*(6), 51641. https://doi.org/10.1002/app.51641
2. Sonseca A, Peponi L, Sahuquillo O, Kenny JM, Gimenez E. (2012). Electrospinning of biodegradable polylactide/hydroxyapatite nanofibers: Study on the morphology, crystallinity structure and thermal stability. *Polymer Degradation and Stability, 97*(10), 2052–2059. https://doi.org/10.1016/j.polymdegradstab.2012.05.009
3. Songling C, YangM, Ba C, Yu S, Jiang Y, Zou H, Zhang Y. (2018). Preparation and characterization of slow-release fertilizer encapsulated by biochar-based waterborne copolymers. *Science of The Total Environment*, *615*, 431–437. https://doi.org/10.1016/j.scitotenv.2017.09.209
4. Liang D, Du C, Ma F, Shen Y, Wu K, Zhou J. (2019). Interaction between polyacrylate coatings used in controlled-release fertilizers and soils in wheat-rice rotation fields. *Agriculture, Ecosystems & Environment*, *286*, 106650. https://doi.org/10.1016/j.agee.2019.106650
5. Reneker DH, Yarin AL, Fong H. (2000). bending instability of electrically charged liquid jets of polymer solutions in electrospinning. *Journal of Applied Physics*, *87*, 4531–4547. https://doi.org/10.1063/1.373532
6. Ghanmi I, Slimani F, Ghanmi S and Guedri M. (2024). Development and characterization of a PLA biocomposite reinforced with date palm fibers. *Engineering, Technology & Applied Science Research*, *14*(2), 13631–13636. https://doi.org/10.48084/etasr.6988
7. Qi H, Ma R, Shi C, Hu Z, Liu S, Sun L, Hu T. (2019). Novel low-cost carboxymethyl cellulose microspheres with excellent fertilizer absorbency and release behavior for saline-alkali soil. *International Journal of Biological Macromolecules, 131*, 412–419. https://doi.org/10.1016/j.ijbiomac.2019.03.047
8. Deng H, Wei G, Li EJ, Ge L, Lai X, Huang Q. (2018). An overflow intelligent early-warning model based on downhole parameters measurement. *International Conference on Image and Video* https://doi.org/10.1117/12.2514042
9. Díaz JE, Fernández-Nieves A, Barrero A, Márquez M, Loscertales IG. (2008). Fabrication of structured micro and nanofibers by coaxial electrospinning. *Journal of Physics: Conference Series 127*, 012008. https://doi.org/10.1088/17426596/127/1/012008
10. Perez JJ, Francois NJ. (2016). Chitosan-starch beads prepared by ionotropic gelation as potential matrices for controlled release of fertilizers. *Carbohydrate Polymers*, *148*, 134–142. https://doi.org/10.1016/j.carbpol.2016.04.054
11. Silva Junior JS, Botta SB, Ana PA, Franca CM, Fernandes KPS, Ferrari RAM, Deana A, Busadori SK. (2015). Effect of papain-based gel on type I collagen - spectroscopy applied for microstructural analysis. *Scientific Reports 5,* 11448, 1–7. https://doi.org/10.1038/srep11448
12. Kumar KK, Jenifer M, Nandhini TJ, Sridharan M, Sabarinathan G, Shanthappa PM. (2025). Molecular insights into the structural, spectroscopic, chemical shift characteristics, and molecular docking analysis of the carbamate insecticide fenobucarb. *Chemical Physics Impact*, *10*, 1–12. https://doi.org/10.1016/j.chphi.2025.100822
13. Sperling LE, Ries KP, Pranke P, Wendorff JH.

(2016). Advantages and challenges offered by biofunctional core–shell fiber systems for tissue engineering and drug delivery. *Drug Discovery Today, 21*(8), 1243–1256. https://doi.org/10.1016/j.drudis.2016.04.024

14. Yin L, Yang S, He M, Chang Y, Wang K, Zhu Y, Liu Y, Chang Y, Yu Z. (2017). Physicochemical and biological characteristics of BMP-2/IGF-1-loaded three-dimensional coaxial electrospun fibrous membranes for bone defect repair. *Journal of Materials Science: Materials in Medicine*, *28*(6), *94*. https://doi.org/10.1007/s10856-017-5898-3
15. Okutan N, Terzi P, Altay F. (2014). Affecting parameters on electrospinning process and characterization of electrospun gelatin nanofibers. *Food Hydrocolloids, 39,* 19–26. https://doi.org/10.1016/j.foodhyd.2013.12.022
16. Bauquier SH, Jiang JL, Yue Z, Lai A, Chen Y, Moulton SE, McLean KJ, Vogrin S, Halliday AJ, Wallace G, Cook MJ. (2016). Antiepileptic Effects of Lacosamide Loaded Polymers Implanted Subdurally in GAERS. *International Journal of Polymer Science*, *2016*(1). https://doi.org/10.1155/2016/6594960
17. Sushila S, Seema S, Pankaj S, Parvesh D, Monika M. (2021). Nanotechnology for sustainable agriculture: An emerging perspective. *Journal of Nanoscience and Nanotechnology*, *21*(6), 3453–4365. https://doi.org/10.1166/jnn.2021.19012
18. Nguyen TTT, Ghosh C, Hwang SG, Chanunpanich N, Park JS. Porous core/sheath composite nanofibers fabricated by coaxial electrospinning as a potential mat for drug release system. *International Journal of Pharmaceutics, 439*(1–2), 296–306 (2012) https://doi.org/10.1016/j.ijpharm.2012.09.019
19. Singh YP, Dasgupta S, Nayar S, Bhaskar R. (2020). Optimization of electrospinning process & parameters for producing defect-free chitosan/polyethylene oxide nanofibers for bone tissue engineering. *Journal of Biomaterials Science, Polymer Edition, 31*(6), 781–803. https://doi.org/10.1080/09205063.2020.1718824